Pax9-deficient mice lack pharyngeal pouch derivatives and teeth and exhibit craniofacial and limb abnormalities

Heiko Peters,[1] Annette Neubüser,[2] Klaus Kratochwil,[3] and Rudi Balling[1,4]

[1]GSF-Research Center for Environment and Health, Institute for Mammalian Genetics, 85764 Neuherberg, Germany; [2]Department of Anatomy and Program in Developmental Biology, University of California, San Francisco, California 94143-0452 USA; [3]Institute of Molecular Biology, Austrian Academy of Sciences, A-5020 Salzburg, Austria

***Pax* genes have been shown to play important roles in mammalian development and organogenesis. *Pax9*, a member of this transcription factor family, is expressed in somites, pharyngeal pouches, mesenchyme involved in craniofacial, tooth, and limb development, as well as other sites during mouse embryogenesis. To analyze its function in vivo, we generated *Pax9* deficient mice and show that *Pax9* is essential for the development of a variety of organs and skeletal elements. Homozygous *Pax9*-mutant mice die shortly after birth, most likely as a consequence of a cleft secondary palate. They lack a thymus, parathyroid glands, and ultimobranchial bodies, organs which are derived from the pharyngeal pouches. In all limbs, a supernumerary preaxial digit is formed, but the flexor of the hindlimb toes is missing. Furthermore, craniofacial and visceral skeletogenesis is disturbed, and all teeth are absent. In *Pax9*-deficient embryos tooth development is arrested at the bud stage. At this stage, *Pax9* is required for the mesenchymal expression of *Bmp4*, *Msx1*, and *Lef1*, suggesting a role for *Pax9* in the establishment of the inductive capacity of the tooth mesenchyme. In summary, our analysis shows that *Pax9* is a key regulator during the development of a wide range of organ primordia.**

[*Key Words: Pax9;* knockout; teeth; palate; thymus; parathyroids; skeleton]

Received March 9, 1998; revised version accepted April 30, 1998.

Pax9 is a member of a transcription factor family that is characterized by a common motif, the DNA-binding paired domain. This motif is encoded by the paired box, a conserved DNA region originally identified in *Drosophila* (Bopp et al. 1986; Baumgartner et al. 1987). In mammals, nine different *Pax* genes, which fall into four different subgroups, have been isolated (Walther et al. 1991; Wallin et al. 1993; Stapleton et al. 1993). Spontaneous as well as targeted mutations in several *Pax* genes have revealed that *Pax* genes perform essential functions during mammalian embryonic development. A common feature of *Pax* mutants is size reduction, malformation, or even the loss of specific organs, such as the immune system, brain, eye, nose, kidney, pancreas, as well as the skeleton and neural crest cell derivatives (for review, see Chalepakis et al. 1993; Dahl et al. 1997 and references therein).

The *Pax9* gene is highly homologous to *Pax1* and is present in all vertebrates analyzed so far, including zebrafish, chick, mouse, and man (Stapleton et al. 1993; Neubüser et al. 1995; Peters et al. 1995; Nornes et al. 1996). During mouse development, *Pax9* and *Pax1* are expressed in a similar, but not identical pattern in the sclerotomes, the ventromedial compartment of the somites that forms the vertebral column. Both genes also exhibit overlapping expression patterns in the endodermally derived epithelium of the pharyngeal pouches, which give rise to the thymus, parathyroid glands, ultimobranchial bodies, eustachian tube, and tonsils. In the limbs, *Pax1* and *Pax9* transcripts localize to adjacent nonoverlapping mesenchymal domains whereas *Pax9*, but not *Pax1*, is widely expressed in neural crest-derived mesenchyme involved in craniofacial and tooth development (Deutsch et al. 1988; Timmons et al. 1994; Neubüser et al. 1995, 1997).

The complex expression pattern of *Pax9* during mouse embryogenesis suggests that it plays a role in the formation of various organs. To investigate its developmental function, we disrupted the murine *Pax9* gene by homologous recombination in ES cells and introduced the resulting mutation into the mouse germ line. Heterozygous mutants exhibit no obvious defects indicating that *Pax9* is haploid sufficient. However, mice homozygous for the *Pax9* deletion die shortly after birth and exhibit a wide range of developmental defects. They lack the derivatives of the third and fourth pharyngeal pouches, that is, the thymus, parathyroid glands, and ultimobranchial

[4]Corresponding author.
E-MAIL balling@gsf.de; FAX 89 3187-3099.

bodies. In addition, all teeth are absent, and our analysis suggests that BMP4-mediated signaling in the tooth mesenchyme is affected in *Pax9*-deficient embryos. The secondary palate is cleft and a variety of skeletal abnormalities affecting the head and the visceral skeleton develop in the absence of *Pax9*. Furthermore, supernumerary digits are formed and the flexor of the hindlimb toes is missing. Taken together, our analysis reveals essential roles for *Pax9* during the development of a variety of organs derived from endoderm, mesoderm, and neural crest.

Results

Generation of Pax9-*deficient mice*

A functional null allele of *Pax9* was created by replacement of the endogenous start codon as well as the exon containing the paired box with a promoterless *Escherichia coli* ATG–*lacZ*–poly(A) cassette and the *PGK–neo* gene (Fig. 1A). ES cells carrying the mutated allele, $Pax9^{lacZ}$, were introduced into mouse blastocysts, and germ-line transmission was obtained from two chimeras (Fig. 1B,C). Heterozygous $Pax9^{lacZ}$ mice are viable, fertile, and do not exhibit any obvious abnormalities. Heterozygous matings gave rise to all expected genotypes at Mendelian frequency (19.7% +/+, 57.2% +/−, 23.1% −/−; n = 173), indicating that lack of Pax9 protein, which was confirmed by Western blot analysis (Fig. 1D), does not result in embryonic lethality. In contrast, newborn *Pax9*-deficient mice exhibit gasping respirations, develop a bloated abdomen (Fig. 1E), and die within few hours.

Expression of the Pax9^{lacZ} *allele*

The normal development of heterozygous $Pax9^{lacZ}$ mutant mice allowed us to use the *lacZ* gene as a sensitive reporter of *Pax9* promoter activity during mouse embryogenesis. X-gal staining of heterozygous $Pax9^{lacZ}$ embryos recapitulated the *Pax9*-expression pattern obtained previously by RNA in situ hybridization studies (Neubüser et al. 1995; A. Neubüser, unpubl.). At E9.0, $Pax9^{lacZ}$ expression was restricted to the pharyngeal pouches (Fig. 2A). At E10.5, additional staining was detected in the somites, in the developing medial nasal process, and at the tip of the tail (Fig. 2B, and data not shown). Cross sections showed that in the somites, the expression is restricted to the ventrolateral part of the sclerotomes whereas, in the tail region, it is confined to the tail gut (Fig. 2B, and data not shown). At E12.0, the mesenchyme of the maxillary and mandibular arches as well as the nasal mesenchymes strongly express $Pax9^{lacZ}$ (Fig. 2C). At E13.5, expression was found in the midbrain, facial mesenchyme, middle ear, pharyngeal epithelium and its derivatives, esophagus, limbs, vertebral column, intercostal mesenchyme, tail gut, and ventral tail mesenchyme (Fig. 2D). In the midbrain, $Pax9^{lacZ}$ expression was detected in the tegmentum and in the developing mammillary bodies (Fig. 2E). At E16.5, $Pax9^{lacZ}$ is expressed in the salivary glands, tongue, and in the mesenchyme of all teeth (Fig. 2F,G,H). At the same stage, the thymus, parathyroid glands, and ultimobranchial bodies, as well as the epithelia of the larynx, esophagus, and forestomach were stained (Fig. 2I).

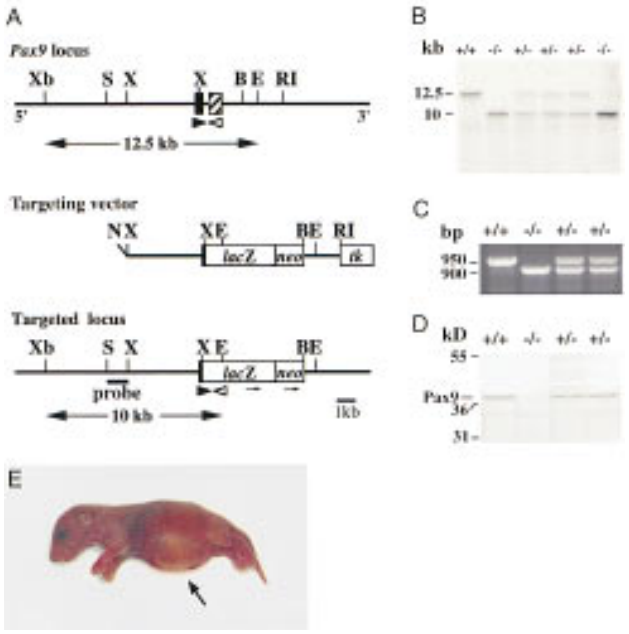

Figure 1. Generation of *Pax9*-deficient mice. (*A*) Structure of wild-type locus, targeting vector, and disrupted *Pax9* allele. The ATG–*lacZ*–*neo* cassette was fused to the ATG-containing exon (black box) of *Pax9*, thereby deleting two thirds of the *Pax9* coding sequence including the DNA binding region encoded by the paired box (hatched box). HSV–TK was ligated to the 3′ arm of the targeting vector and was used as a negative selection marker. The 5′ external probe used for genomic Southern blot analysis is shown as a black line. Solid arrowheads indicate the primer located in the ATG-containing exon; open arrowheads indicate allele-specific primers that were used for genotyping. (B) *Bgl*II; (E) *Eco*RV; (N) *Not*I; (RI) *Eco*RI; (S) *Sal*I; (X) *Xma*I; (Xb) *Xba*I. (*B*) Southern analysis of embryos obtained by heterozygote matings. (*C*) PCR assay of $Pax9^{lacZ}$ mutant embryos. Yolk sacs of embryos were used for isolation of genomic DNA. PCR was performed with three primers shown in *A* in a single reaction to distinguish between the wild-type (950 bp) and the transgenic (900 bp) locus. (*D*) Western blot analysis of $Pax9^{lacZ}$ mutant embryos. The antiserum 281-IV detects a Pax9-specific 38-kD band only in protein extracts prepared from vertebral columns of wild-type and heterozygous embryos (E13.5). (*E*) Homozygous $Pax9^{lacZ}$ mutant shortly after birth. The mutants are born alive but die within a few hours. During that time, they exhibit gasping respirations and develop a bloated abdomen (arrow).

In the following description, we refer to homozygous $Pax9^{lacZ}$ mutant mice as mutants whereas controls are either wild type or heterozygous.

Formation of a cleft secondary palate in Pax9-*deficient mice*

Inspections of the head revealed that all mutants have a cleft secondary palate at birth, thus providing a possible explanation for the severe respiratory problems observed

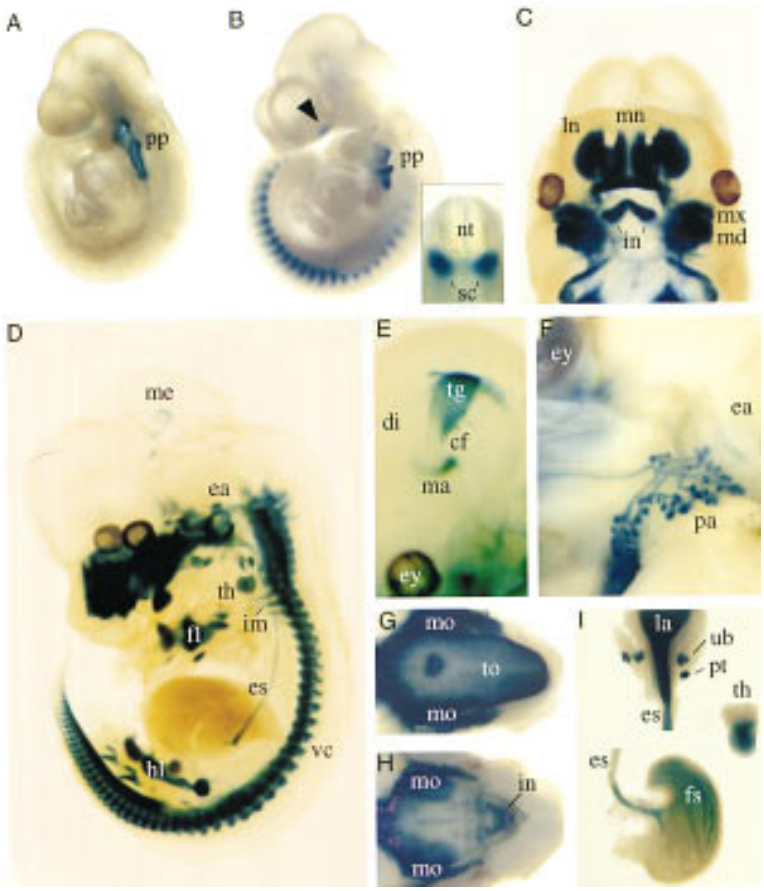

Figure 2. Expression of the $Pax9^{lacZ}$ allele during mouse development revealed by whole-mount X-gal staining of heterozygous $Pax9^{lacZ}$ embryos. (*A*) $Pax9^{lacZ}$ expression at E9.0 is restricted to the pharyngeal pouches (pp). (*B*) At E10.5, additional staining is detectable along the body axis and in the facial mesenchyme (arrowhead). The expression in the somites is restricted to the sclerotomes (sc in insert). (*C–E*) Embryos were cleared with benzylbenzoate/benzylalcohol after X-gal staining. (*C*) At E12.0, mesenchymes of the nasal processes as well as of the maxillary (mx) and mandibular (md) arches are strongly stained. In addition, expression of $Pax9^{lacZ}$ is seen in the region of the developing lower incisors (in). (*D*) At E13.5, a number of structures express $Pax9^{lacZ}$ including facial mesenchyme, ear (ea), thymus (th), esophagus (es), forelimb (fl), hindlimb (hl), vertebral column (vc), intercostal mesenchyme (im), and a small domain of the mesencephalon (me). (*E*) In the mesencephalon, $Pax9^{lacZ}$ expression is restricted to the tegmentum (tg) and the mammillary bodies (ma) at E14.5. (*F–I*) $Pax9^{lacZ}$ expression at E16.5. (*F*) Lateral view of the head. The branching ducts of the parotis gland (pa) are $Pax9^{lacZ}$ positive. (*G*) In the lower jaw, $Pax9^{lacZ}$ expression was found in the tongue (to) and in the region of the developing molars (mo). (*H*) Similarly, the expression in the upper jaw is strongest in the region of the developing teeth. (*I*) The derivatives of the foregut endoderm express $Pax9^{lacZ}$. Expression was detected in the epithelium of the larynx (la), esophagus (es), and forestomach (fs), but also in the thymus (th), parathyroid glands (pt), and ultimobranchial bodies (ub). (cf) Cephalic flexure; (di) diencephalon; (ey) eye; (ln) lateral nasal process; (mn) medial nasal proces; (nt) neural tube.

in those pups. Skeletal stainings revealed that both maxillary and palatine shelves are cleft, allowing direct view to the presphenoid and into the nasal cavity (Fig. 3G).

To examine the developmental course of cleft palate formation, different stages of embryonic development were analyzed histologically. Secondary palate formation starts around E12.0 with a bilateral outgrowth from the maxillary portions of the first branchial arch. The palatal processes grow along the side of the tongue and later elevate and fuse above the dorsum of the tongue (Greene and Pratt 1976). At E12.0, the palatal shelves of mutant embryos appear normal compared to those of control embryos (data not shown). In contrast, at E13.5 the shelves of mutant embryos revealed an abnormally broadened shape and lacked characteristic indentations at their ventrolateral sides (Fig. 3C). At this stage, *Pax9* is normally expressed not only in the palatal shelves, but also in the mesenchyme of the mandibular arch facing the palatal shelves (Fig. 3A). This region of the mandible is also abnormally shaped in the mutant (Fig. 3C). The aberrant morphology of the palatal shelves suggests that in mutant embryos, the simultanous elevation, a prerequisite for normal palate development, is mechanically hindered. In fact, we have observed mutant embryos in which shelf elevation has occurred only on one side (Fig. 3E). Therefore, *Pax9* is not necessary for the capability of the shelves to elevate but is required to regulate their shape at a critical stage of secondary palate formation.

Tooth development is arrested at the bud stage in the absence of Pax9

Previous studies have demonstrated that, in the mandibular arch, *Pax9* is expressed in prospective tooth mesenchyme prior to any morphological signs of odontogenesis and that *Pax9* expression is restricted to the mesenchymal compartment of the developing teeth between E10.0 and E16.5 (Fig. 3A; Neubüser et al. 1997; and A. Neubüser, unpubl.). Inspections of both jaws of newborn *Pax9* mutant mice revealed the absence of all teeth. To investigate at which stage tooth development is affected, we followed molar development in mutant and control embryos in serial histological sections. By morphological criteria, tooth development is initiated normally in the mutant and is indistinguishable from controls until E12.5 (data not shown). At E13.5, the dental epithelia of both mutants and controls have invaginated to form epithelial buds, but the condensation of mesenchymal cells around the bud is less prominent in the mutant (Fig. 4A,B). At E14.5, tooth development has reached the cap stage in wild-type embryos whereas, in mutants, only a rudimentary bud was present (Fig. 4C,D). Examination of

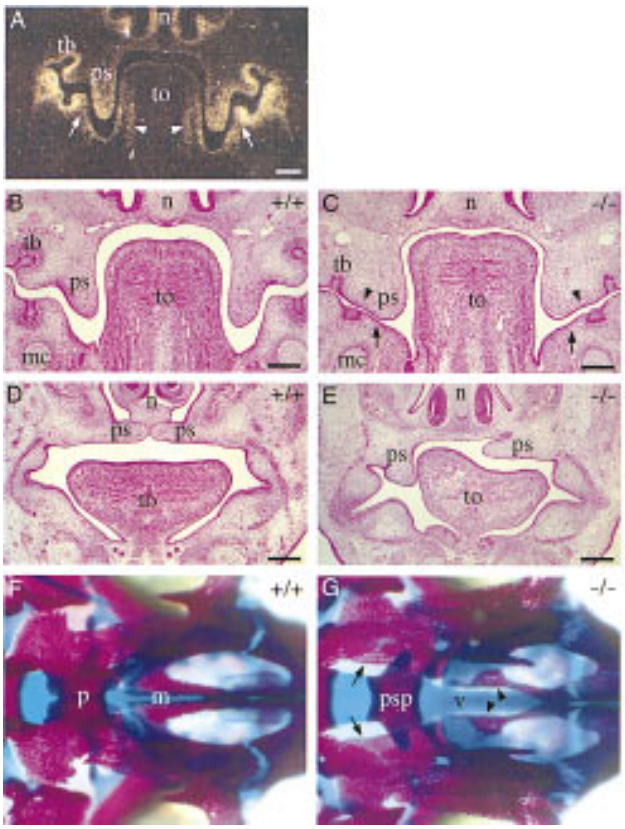

Figure 3. Development of cleft secondary palate in homozygous *Pax9*^{lacZ} mutant embryos. (*A–C*) Coronal section of the head at the level of the developing molars at E13.5. (*A*) Section hybridized with a *Pax9*-specific RNA probe. *Pax9* is expressed in the mesenchymes of the nose (n), palatal shelves (ps), and in the mesenchyme underlying the epithelial tooth bud (tb). Note also the expression of *Pax9* in the mandibular arch mesenchyme facing the palatal shelves (arrows) and in the lateral tongue (to) mesenchyme (arrowheads). (*B*) H/E-stained section of a wild-type embryo. (*C*) H/E-stained section of a homozygous *Pax9*^{lacZ} embryo. The palatal shelves are present but abnormally broadened. Both lateral indentations of the palatal shelves (arrowheads) as well as the mesenchymal outgrowth (arrows) facing the indentations are absent. (*D,E*) H/E-stained coronal sections anterior to the developing molars at E14.5. (*D*) In wild-type embryos, palatal shelves have elevated and are in the process of fusion. (*E*) In *Pax9*-deficient embryos, bilateral shelve elevation is impaired. (*F,G*) Skeletal stainings of the secondary palate of newborn mice. Anterior is to the *right*. (*F*) In wild-type mice the bony elements of the palatine (p) and the maxillary (m) shelves are almost fused. (*G*) In homozygous *Pax9*^{lacZ} mutants both shelves are absent allowing direct view to the vomer (v) and the presphenoid (psp). The borders of the open maxillary and palatine shelves are indicated by arrowheads and arrows, respectively. (mc) Meckels cartilage. Bars, 200 µm.

later stages revealed that tooth development never proceeded beyond the bud stage (data not shown). Thus, *Pax9* function is required in all developing teeth before or at the bud stage (E13.5).

Tooth development is characterized by a series of interactions between dental epithelium and mesenchyme. Odontogenesis is induced by the epithelium around E10.0 whereas between E11.5 and E13.5, the mesenchyme becomes the dominating tissue (Mina and Kollar 1987; Lumsden 1988; for review, see Thesleff and Sharpe 1997). Although the tooth buds of *Pax9*-deficient embryos appeared histologically normal, they may already be affected by the absence of *Pax9* expression before E13.5. To investigate whether the potential of epithelial morphogenesis is irreversibly lost in the tooth buds of *Pax9*-deficient embryos, we performed tissue recombination experiments. Epithelia and mesenchymes from tooth germs of normal and *Pax9*-deficient embryos at E13.5 were separated, reassociated in both combinations and were then grafted under kidney capsules of adult mice. Combinations of *Pax9*-deficient mesenchyme and normal epithelium (both E13.5) formed epithelial cysts only and failed to form teeth ($n = 6$, data not shown). However, combinations of normal mesenchyme with *Pax9*-deficient epithelium yielded at least one tooth per graft ($n = 6$). Furthermore, tooth morphogenesis was similar to that of control combinations, and both tissues completed cytodifferentiation including the secretion of dentin and enamel (Fig. 4E,F). These results show that *Pax9* function is required in the mesenchyme but also demonstrates that all consequences of *Pax9* deficiency on epithelial development before E13.5 can be overcome by a wild-type mesenchyme isolated at the bud stage.

Pax9 *is required for the mesenchymal expression of* Bmp4, Msx1, *and* Lef1 *at a critical stage of tooth development*

At the bud stage, the tooth mesenchyme induces the formation of the epithelial enamel knot, a signaling center that regulates tooth development at the cap stage (Vaahtokari et al. 1996). Recently, BMP4 was shown to be involved in this induction (Jernvall et al. 1998). At E13.5, *Bmp4* is expressed in tooth mesenchyme, and recombinant BMP4 was found to induce mesenchymal expression of *Msx1*, *Lef1*, and *Bmp4* itself (Vainio et al. 1993; Kratochwil et al. 1996). Conversely, mesenchymal *Bmp4* expression depends on *Msx1* (Chen et al. 1996), but not on *Lef1* (Kratochwil et al. 1996), two other genes required for tooth development to proceed beyond the bud stage (Satokata and Maas 1994; Van Genderen et al. 1994). To determine whether *Pax9* is involved in the regulation of these genes, we analyzed the expression of *Bmp4*, *Msx1*, and *Lef1* in tooth primordia of mutant embryos. At E12.0, the expression patterns of all three genes in mutant embryos were indistinguishable from those of wild-type embryos (data not shown). At E13.5, however, *Bmp4* expression was barely detectable in the mesenchyme of *Pax9*^{lacZ} mutant embryos (Fig. 4H). At the same stage, the mesenchymal expression of *Msx1* and *Lef1* was found to be substantially down-regulated (Fig. 4J,L). At E14.5, both *Msx1* and *Lef1* transcripts were present in the tooth mesenchyme of controls but were almost undetectable in the mutants (data not shown). These results demonstrate that, at the bud stage, *Pax9* is required for the maintenance of *Bmp4* expression in the

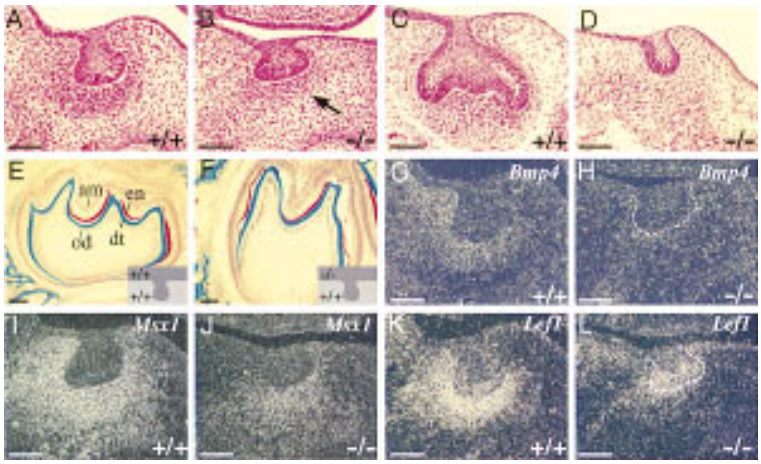

Figure 4. Arrest of tooth development in homozygous $Pax9^{lacZ}$ mutant embryos. (*A–D*) H/E-stained coronal sections at the level of the developing molars. (*A*) At E13.5, mesenchymal cells condense around the epithelial tooth bud. (*B*) At the same stage, in the homozygous $Pax9^{lacZ}$ mutant embryo, a tooth bud has formed but cellular condensation is reduced (arrow). (*C*) At E14.5, tooth development has reached the cap stage in the wild-type embryo. (*D*) In contrast, loose mesenchyme underlying a rudimentary bud is present in the mutant littermate. (*E,F*) Tooth development in experimental combinations of dental tissues isolated at E13.5. (*E*) Combinations of wild-type dental mesenchyme and wild-type epithelium yielded well-developed teeth in subrenal grafts. Typical cytodifferentiation was observed including the presence of dentine (dt) secreted by odontoblasts (od), and enamel (en) secreted by ameloblasts (am). (*F*) A similar result was obtained with normal mesenchyme combined with *Pax9*-deficient dental epithelium. In contrast, combinations of *Pax9*-deficient mesenchyme and normal epithelium failed to form teeth (data not shown). (*G–L*) In situ hybridization of mesenchymal markers during molar development of normal (*G,I,K*) and *Pax9* mutant (*H,J,L*) embryos at E13.5. (*G*) At E13.5, *Bmp4* is expressed in the mesenchyme underlying the epithelial tooth bud. In the absence of *Pax9* (*H*), *Bmp4* transcripts are barely detectable. (*I*) *Msx1* expression is strong in the tooth mesenchyme and substantially reduced in the absence of *Pax9* (*J*). (*K*) In wild-type embryos, both the mesenchyme and the margin of the tooth bud epithelium express *Lef1*. (*L*) In the absence of *Pax9*, the mesenchymal expression of *Lef1* is reduced whereas the expression in the epithelium is not affected. For clarity, the borders of the tooth buds are outlined by broken lines in *H* and *L*. Bars, 100 μm.

dental mesenchyme, which provides a possible explanation for the subsequent down-regulation of *Msx1* and *Lef1* expression.

Pax9 *is essential for the development of thymus, parathyroid glands, and ultimobranchial bodies*

To investigate the role of *Pax9* during the formation of organs derived from the pharyngeal pouches, serial histological sections of the neck and upper trunk region of mutant embryos (E14.5) were analyzed. No developmental abnormalities were found in the derivatives of the first and second pouches (data not shown). In contrast, the primordia of thymus and parathyroid glands, both derivatives of the third pharyngeal pouches, as well as the ultimobranchial bodies, which are derived from the fourth pouches, are absent in *Pax9*-deficient embryos (Fig. 5D,J,N). To determine the onset of phenotypic abnormalities during pharyngeal pouch development, we used X-gal staining of heterozygous and homozygous $Pax9^{lacZ}$ mutant embryos to label the pharyngeal pouch epithelia.

At E10.0, the pharyngeal pouches, outlined by $Pax9^{lacZ}$-expression appear normal in homozygous mutant embryos (Fig. 5F) indicating that the initial phase of pharyngeal pouch formation is not disturbed. In contrast, at E11.5, development of the third and fourth pharyngeal pouches is retarded in mutant embryos (Fig. 5H). Subsequently, these pouches do not separate as epithelial buds to form the early rudiments of thymus, parathyroids, and ultimobranchial bodies (Fig. 5J). At E14.5, the primordia of thymus, parathyroid glands, and ultimobranchial bodies were clearly visible in heterozygous embryos (Fig. 5M), whereas none of these organs could be detected in homozygous mutants (Fig. 5N). Because the fourth pharyngeal pouches are difficult to identify on histological sections, we used *HoxB1* expression as an early marker of the fourth pharyngeal pouch epithelium (Frohman et al. 1990; Manley and Capecchi 1995). Immunostaining revealed that at E10.0, expression of HoxB1 in mutant embryos was indistinguishable from that of controls (Fig. 5K,L). By E11.0, however, HoxB1 expression in the mutants was strongly reduced (Fig. 5P), supporting our conclusion that ultimobranchial bodies are not formed in the absence of *Pax9*.

Pax9 *is required for skeletal development of skull and larynx*

In situ hybridizations to horizontal sections of the head (E14.0) showed that *Pax9* is expressed at the base of the developing skull (Fig. 6B). Skeletal preparations revealed the absence of the processus alaris in the skull of newborn mutants (Fig. 6D). In addition, the pterygoid process is severely malformed and, in most cases, the tympanic ring is greatly reduced in size (Fig. 6D,H). In both jaws, the alveolar ridges, which normally surround molars and incisors, are missing (Fig. 6K and data not shown). Moreover, the coronoid process, a dorsal extension of the mandible, is absent (Fig. 6K).

At E14.0, expression of $Pax9^{lacZ}$ was detected in the mesenchyme surrounding Reicherts cartilage (Fig. 6E). In most mutants, Reicherts cartilage was absent (Fig. 6F,H); however, in a few cases (3/26), it was extended and connected to the hyoid bone (Fig. 6I). In the laryngeal cartilages of homozygous mutants, both the greater and the lesser horn of the hyoid bone are malformed. In addition, the thyroid cartilage is broadened and lacks two processes normally connecting thyroid and cricoid cartilage (Fig. 6M). Remarkably, we were not able to detect *Pax9*

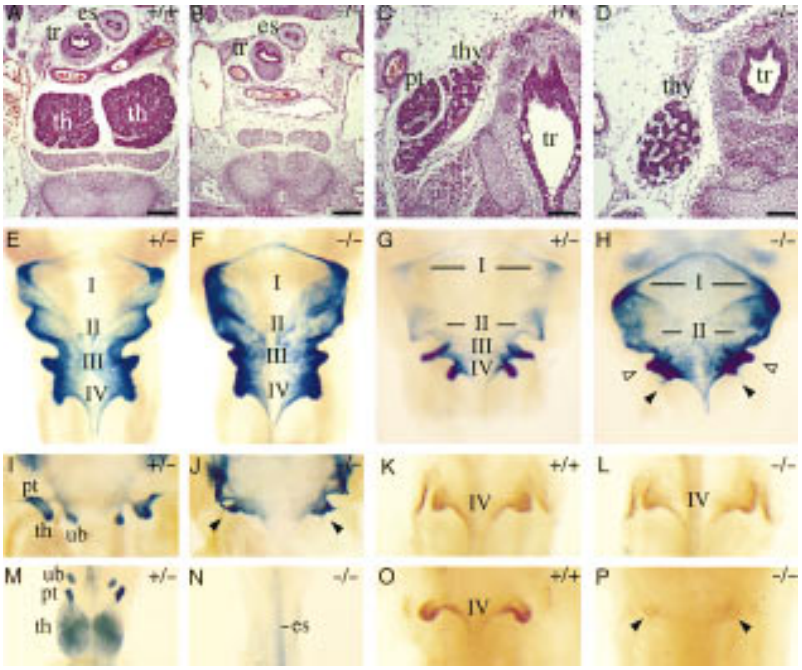

Figure 5. Absence of thymus, parathyroid glands, and ultimobranchial bodies in *Pax9*-deficient mice. (*A–D*) H/E-stained transverse sections of the neck region at E14.5. (*A*) Two thymic lobes (th) are present in the wild-type embryo. (*B*) At the same level, *Pax9*-deficient embryos are completely devoid of the thymus. Thymic rudiments were also not found in other regions of the neck and upper trunk (data not shown). (*C*) The parathyroid glands (pt) are attached to the thyroid gland (thy) in wild-type embryos and are absent in homozygous $Pax9^{lacZ}$ mutant embryos (*D*). (*E–J,M,N*) Ventral view of cleared whole-mount X-gal stainings of the pharyngeal pouches and their derivatives in $Pax9^{lacZ}$ mutant embryos. (*E*) In heterozygous $Pax9^{lacZ}$ mutant embryos at E10.0, $Pax9^{lacZ}$ is expressed in all four pharyngeal pouches (I–IV). (*F*) At the same stage, the third and fourth pharyngeal pouches are also present in homozygous $Pax9^{lacZ}$ mutant embryos. (*G*) The third and fourth pharyngeal pouches have started to separate from the pharynx epithelium at E11.5. (*H*) In homozygous $Pax9^{lacZ}$ mutants, the third (open arrowheads) and fourth (filled arrowheads) pouches are retarded at E11.5. (*I*) Around E12.0, individual organ primordia of thymus (th), parathyroid glands (pt), and ultimobranchial bodies (ub) become visible as epithelial buds, which are absent in homozygous $Pax9^{lacZ}$ mutants (arrowheads in *J*). (*M*) $Pax9^{lacZ}$ expression is maintained in the primordia of thymus, parathyroid glands, and ultimobranchial bodies of heterozygous $Pax9^{lacZ}$ mutant embryos at E14.5, whereas these organs are absent in homozygous $Pax9^{lacZ}$ mutant embryos (*N*). (*K,L,O,P*) Ventral view of the fourth pharyngeal pouches of whole-mount embryos stained with HoxB1-specific antibodies. At E10.0, the epithelium of the fourth pouches expresses HoxB1 in both wild-type (*K*) and *Pax9*-deficient (*L*) embryos. (*O*) At E11.5, HoxB1 expression is continued in the fourth pharyngeal pouches. (*P*) A weak expression of HoxB1 (arrowheads) is detectable in the epithelial remnant of the fourth pharyngeal pouches in homozygous $Pax9^{lacZ}$ mutant embryos. (es) Esophagus; (tr) trachea. Bars, 200 μm.

expression in the laryngeal cartilages at any stage (E12.5–E18.5; data not shown).

Skeletal defects of the limbs

In the developing limbs, expression of *Pax9* is first detectable at E11.5 in the anterior mesenchyme of the limb bud (Neubüser et al. 1995; Fig. 7A). Subsequently, the *Pax9* expression domains elongate and are found in the anterior mesenchymes of the zeugopods of fore- and hindlimb at E12.5, as shown by X-gal staining of heterozygous $Pax9^{lacZ}$ mutants (Fig. 7B,C). $Pax9^{lacZ}$ is also expressed in the region of the developing metatarsals and metacarpals (Fig. 7B,C), suggesting that *Pax9* is involved in pattern formation at different sites of the developing limb.

Skeletal preparations reveal that homozygous $Pax9^{lacZ}$ mutants develop preaxial digit duplications in both fore- and hindlimbs. In the hindlimb, a small supernumerary toe is formed (Fig. 7G). In addition, the ossification center of the first phalange is severely reduced in the first toe, and the anterior tarsals are abnormally broadened and fused. The phenotype is less severe in the forelimb in which the supernumerary digit does not separate from the thumb (Fig. 7E). Externally, the first signs of limb malformations were detected around E13.5 as a thickening of the anterior–proximal limb mesenchyme (data not shown).

To examine the limb abnormalities in more detail, we analyzed cross sections of X-gal stained hindlimbs (E14.0). At the mid-level of the metatarsals, $Pax9^{lacZ}$ expression was seen between individual metatarsals in both control and mutant embryos (Fig. 8C,D). At this level, no abnormalities were detected in the mutants. In the proximal region of the metatarsals of control embryos, $Pax9^{lacZ}$-expression is sharply restricted to the region of the developing first metatarsal and ventrally to it. In contrast, in the mutants the expression was found in a wide area of undifferentiated mesenchyme where the additional digit is formed (Fig. 8E,F). This result indicates that *Pax9* regulates pattern formation of the anterior skeletogenic mesenchyme, and that this process in turn is required to restrict *Pax9* expression to the correct sites. In the absence of *Pax9*, additional mesenchyme is formed in the anterior limb region, which later differentiates into supernumerary digits and ectopic cartilage in the middle hand or foot.

At the level of the tibia, $Pax9^{lacZ}$ expression was found to be proximally extended in homozygous mutants (Fig. 8B). Cross sections of controls revealed that in this region $Pax9^{lacZ}$ is expressed in noncartilaginous tissues including two developing tendons (Fig. 8G,I). These ten-

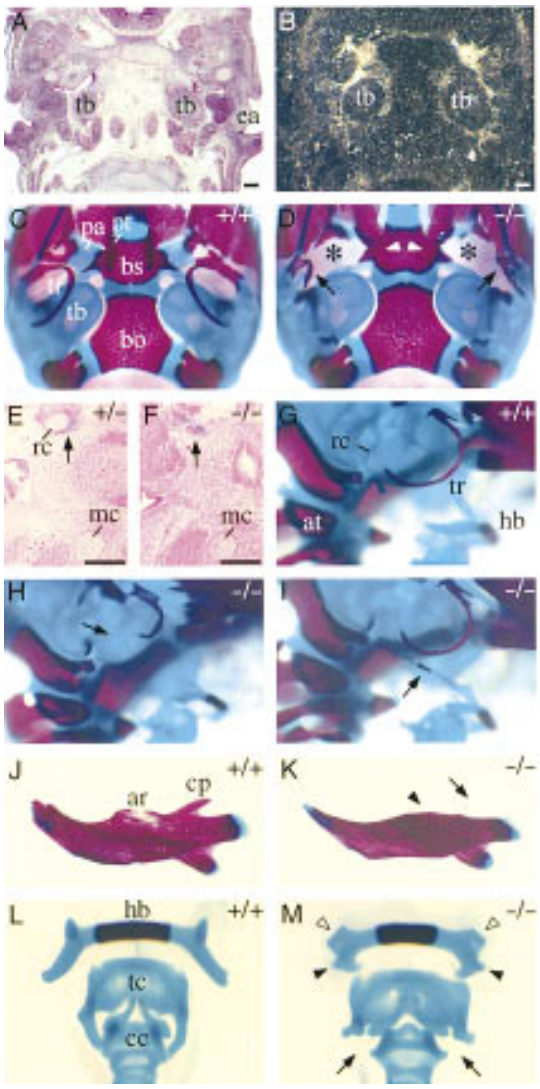

Figure 6. Craniofacial abnormalities in homozygous $Pax9^{lacZ}$ mutant mice. (*A*) H/E-stained section of the base of the developing skull at E13.5. (*B*) Parallel section to *A* hybridized with a *Pax9*-specific RNA probe. Expression of *Pax9* is found in the mesenchyme surrounding the tympanic bulla (tb). (*C*,*D*) Ventral view of the skull stained with alizarin red and alcian blue. Anterior is at the *top* and the lower jaw has been removed. (*C*) Skeletal elements of the posterior half of the skull. (*D*) In homozygous $Pax9^{lacZ}$ mutant mice the processus alaris [(pa) asterisks] is absent and the pterygoid process [(pt) arrowheads] is malformed. Note also the severely malformed tympanic rings (arrows). (*E*) Weak $Pax9^{lacZ}$ expression is detectable in a heterozygous $Pax9^{lacZ}$ mutant at E14.0 in the mesenchyme surrounding Reicherts cartilage (rc). (*F*) In most homozygous $Pax9^{lacZ}$ mutants Reicherts cartilage is absent, however, $Pax9^{lacZ}$ expression is found in a region in which it normally develops (arrow). (*G*–*M*) Skeletal staining of different skeletal elements of newborn mice. (*G*,*H*,*I*) Lateral view of Reicherts cartilage and middle ear. Anterior is to the *right*. (*G*) Normal shape of Reicherts cartilage (rc) in a wild-type newborn mouse. (*H*) In most cases, Reicherts cartilage is not formed in the absence of *Pax9* (arrow). (*I*) In few homozygous $Pax9^{lacZ}$ mutants, Reicherts cartilage is present but abnormally elongated and fused to the hyoid bone (hb). The arrow points to the ossification center of Reicherts cartilage. Note also that in this specimen the tympanic ring (tr) is not affected. (*J*) Normal appearance of the lower jaw. (*K*) In homozygous $Pax9^{lacZ}$ mutants the alveolar ridge [(ar) arrowhead] and the coronoid process [(cp) arrow] are absent. (*L*) Dorsal view of the laryngeal cartilages of normal mice. (*M*) In the absence of *Pax9* both lesser (open arrowheads) and greater (solid arrowheads) horns of the hyoid bone (hb) are malformed. The thyroid cartilage (tc) of the mutant is broadened and lacks lateral processes normally connecting thyroid and cricoid cartilage [(cc) arrows]. (at) Atlas; (bo) basioccipital bone; (bs) basisphenoid; (ea) ear; (mc) Meckels cartilage. Bars, 200 µm.

dons belong to a group of three muscles located at the ventral side of the tibia (Fig. 8M). Cross sections through the leg of mutant embryos not only confirmed the ectopic expression of $Pax9^{lacZ}$ ventrally to the tibia, but also revealed the absence of one of the three tendons (Fig. 8H,J). Sections through the lower leg of newborn mice indicated that the missing tendon belongs to the musculus flexor digitorum, the flexor of the second to fifth toes (Fig. 8K,L), which itself is also absent in homozygous mutant mice (Fig. 8N). In contrast, no abnormalities were detectable in the musculature of the forelimbs of mutant mice (data not shown).

Discussion

In this study we have analyzed the developmental role of *Pax9* in vivo. The phenotype of homozygous $Pax9^{lacZ}$ mouse mutants revealed an essential function of this gene in the development of a wide range of organs and skeletal elements (Table 1). *Pax9* is required for the formation of thymus, parathyroid glands, and ultimobranchial bodies, organs of endodermal origin. An essential role of *Pax9* in organs derived from neural crest mesenchyme was shown by the absence of teeth and the formation of a cleft secondary palate in *Pax9*-deficient mice. Skeletal defects at the base of the skull indicate an involvement of *Pax9* in the development of derivatives of the prechordal plate mesoderm. Finally, in the limbs *Pax9* is required for normal development of the skeleton and musculature, which are formed by the lateral plate and paraxial mesoderm, respectively. Thus, *Pax9* is a key regulator of organogenesis at diverse sites of the mammalian embryo, and its function is neither restricted to a specific germ layer nor to a specific cell type.

The role of Pax9 *during tooth development*

In the mesenchyme of the first branchial arch, the level of *Pax9* expression is highest in the immediate vicinity of the epithelia, suggesting an involvement of *Pax9* in epithelial–mesenchymal interactions (Neubüser et al. 1997). During tooth development, FGF8, a member of

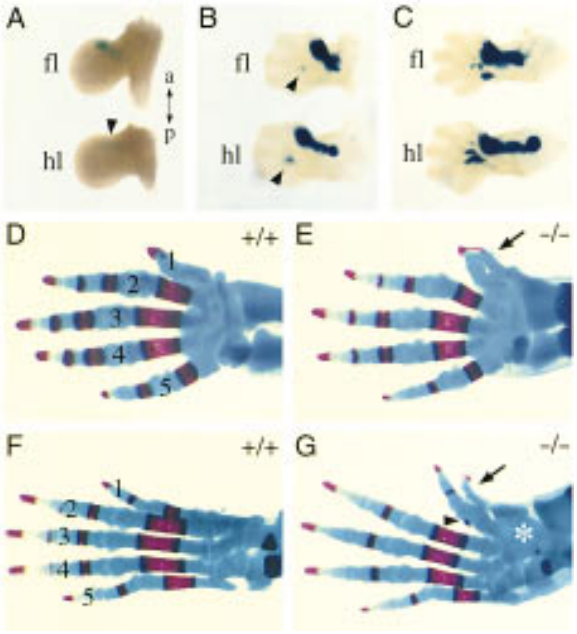

Figure 7. Preaxial digit duplications of hind- and forelimb in *Pax9*-deficient mice. (*A*,*B*,*C*) $Pax9^{lacZ}$ expression during limb development in heterozygous $Pax9^{lacZ}$ mutants. The dorsal view of the left limbs is shown and the anterior–posterior (a,p) axis is indicated. (*A*) At E11.5, $Pax9^{lacZ}$ expression is seen in an anterior domain of the forelimb (fl) whereas at this stage the expression in the hindlimb (hl) is only weakly detectable (arrowhead). (*B*) At E12.5 the expression domain is elongated and expression starts in the region of the middle hand/foot. (*C*) Distinct patches of $Pax9^{lacZ}$ expression appear in the middle hand/foot at E13.5 and the expression in both zeugopods is maintained. (*D*–*G*) Skeletal stainings of the left fore- (*D*,*E*) and hindlimbs (*F*,*G*) of newborn wild-type (*D*,*F*) and homozygous $Pax9^{lacZ}$ mutants (*E*,*G*). Dorsal views are shown and the digits are numbered. (*E*) In the forelimb the extra-formed digit (arrow) is not separated from the thumb. (*G*) In the hindlimb of homozygous $Pax9^{lacZ}$ mutants the duplication of the first digit (arrow) is accompanied by an enlarged cartilaginous area in the region of the anterior metatarsals (asterisk). Note also the abnormal ossification center in the first toe (arrowhead).

the fibroblast growth factor family is expressed in a wide area of the oral epithelium and has been suggested to be the endogenous inducer of *Pax9* expression in mandibular arch mesenchyme. This induction is spatially restricted by BMP4 and/or BMP2, both members of the TGFβ growth factor family. Thus, antagonistic signaling of FGF8 and BMP4/2 is a potential mechanism for positioning the sites of tooth formation in vivo (Neubüser et al. 1997).

Our analysis shows that *Pax9* is essential for tooth development to proceed beyond the bud stage. The first deviation in mutant tooth development is a failure of the mesenchyme to condense around the epithelial bud. This phenotype is remarkably similar to that seen in *Msx1*-deficient mice (Satokata and Maas 1994). *Msx1* and *Pax9* exhibit an overlapping expression pattern in tooth mesenchyme, raising the possibility that both genes act in the same developmental pathway. Experimental evidence indicated that *Msx1* and *Bmp4* expression in the dental mesenchyme are maintained through a positive feedback loop, which might be essential for tooth development to proceed from the bud to the cap stage (Chen et al. 1996). Our results show that this feedback loop is indeed affected in *Pax9*-deficient embryos: At the bud stage, the expression of *Bmp4, Msx1,* and *Lef1* were found to be down-regulated in the tooth mesenchyme of homozygous $Pax9^{lacZ}$ mutants. Thus, at a critical stage of tooth development, *Pax9* may act upstream of *Bmp4, Msx1,* and *Lef1*. Consistent with this idea, preliminary results indicate that mesenchymal *Pax9* expression is not altered in $Msx1^{-/-}$ or $Lef1^{-/-}$ mutant embryos (H. Peters, unpubl.). *Pax9* function might be required to induce the formation of the enamel knot by maintaining the expression of *Bmp4,* which was recently shown to be involved in enamel knot induction (Jernvall et al. 1998). The molecular mechanism of *Pax9* function within this particular network remains to be resolved. Because the early *Msx1* expression (up to E12.0) is not affected in homozygous $Pax9^{lacZ}$ mutants, it is unlikely that *Pax9* is involved in the transcriptional regulation of the *Msx1* gene. Instead, from our data, we favor a model in which the later decline of *Msx1* and *Lef1* expression in homozygous $Pax9^{lacZ}$ mutants is caused by the absence of BMP4 at E13.5.

Pax9 *is required for secondary palate development*

A cleft secondary palate is one of the most frequent birth defects in humans and is generally attributed to a combination of genetic predisposition and environmental factors (Murray 1995; Thorogood 1997). Among environmental factors, certain teratogens such as retinoic acid, ethanol, 6-aminonicotinamide, as well as other substances have been identified as inducers of a cleft secondary palate (Sulik et al. 1988; Gorlin et al. 1990). Recently, it has been suggested that cleft secondary palate formation in mice induced by 6-aminonicotinamide involves genes at the chromosomal region in which *Pax9* is located (Diehl and Erickson 1997). Our analysis has provided genetic evidence that *Pax9* is indeed essential for secondary palate formation, and we have shown that *Pax9* is required to regulate the normal shape of the palatal shelves prior to shelf elevation. Therefore, our findings should help us to understand the effects of teratogens during secondary palate development on the molecular level.

Lack of pharyngeal pouch derivatives

In the absence of *Pax9,* all pharyngeal pouches are initially formed but the development of the third and fourth pouches is arrested at E11.5, leading to the lack of thymus, parathyroid glands, and ultimobranchial bodies. At this stage, not only *Pax9,* but also *Pax1,* is expressed in the epithelium of the third pharyngeal pouches, and it was shown that at later stages, *Pax1* expression in the thymic epithelium is required for normal T-cell maturation (Wallin et al. 1996). However, *Pax1* is apparently not able to compensate for the absence of *Pax9* during the

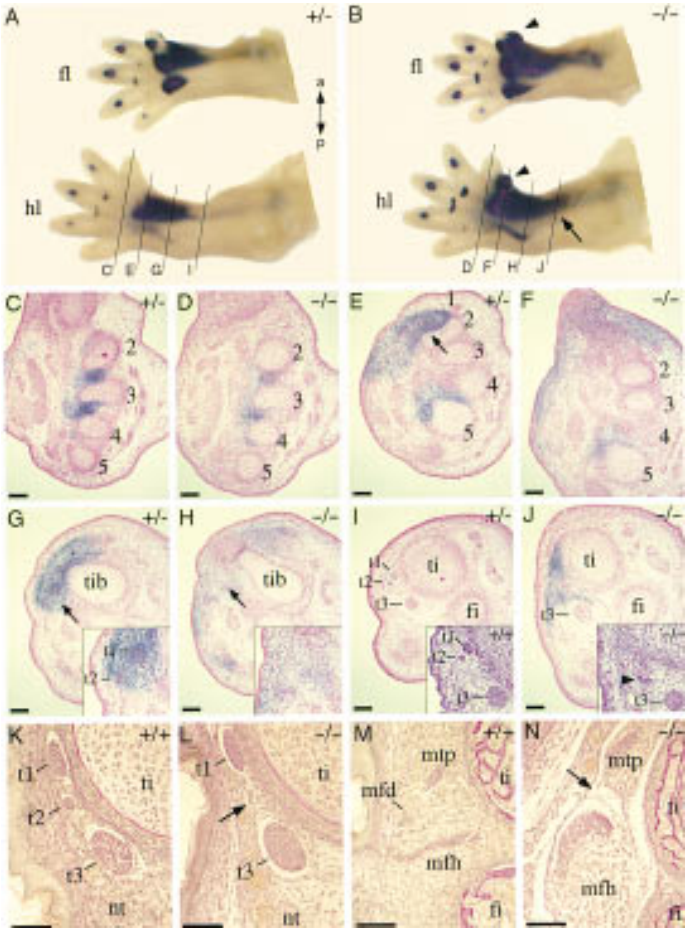

Figure 8. Analysis of the hindlimb defects of homozygous $Pax9^{lacZ}$ mutants. (*A*) $Pax9^{lacZ}$ expression in the fore- (fl) and hindlimb (hl) of a heterozygous $Pax9^{lacZ}$ mutant at E14.0. (*B*) $Pax9^{lacZ}$ expression in a homozygous $Pax9^{lacZ}$ littermate. Note the strong expression in the developing extra-digits (arrowheads) and the proximally extended expression in the hindlimb (arrow). The level of sections in the panels shown below (*C–J*) are indicated in *A* and *B*. (*C–J*) Sections of X-gal-stained *Pax9* mutant embryos (E14.0) counterstained with nuclear red. (*C*) At the level of the middle-foot expression of $Pax9^{lacZ}$ is restricted to the mesenchyme between the metatarsals (2–5). (*D*) A similar expression pattern is seen in the homozygous $Pax9^{lacZ}$ mutant. At the proximal region of the metatarsals the anterior expression domain of $Pax9^{lacZ}$ in the heterozygous mutant (*E*) is restricted (arrow) to a specific region whereas in the absence of *Pax9* (*F*) the expression is distributed in a wide area of undifferentiated mesenchyme. (*G*) At the level of the tibiale (tib), the expression of $Pax9^{lacZ}$ covers the region of two developing tendons in the heterozygous $Pax9^{lacZ}$ mutant (t1 and t2, see arrow and magnification in the *inset*). (*H*) In the homozygous mutant the tendons are not detectable at this level (arrow). (*I*) At the distal end of the tibia, a group of three tendons (t1, t2, t3) are detectable. H/E staining confirmed the same arrangement of these tendons in a wild-type embryo (*inset*). (*J*) In contrast, in homozygous $Pax9^{lacZ}$ mutants, only one tendon (arrowhead in *inset*) is detectable in the region of t1 and t2. Note also the ectopic expression of $Pax9^{lacZ}$ in the region where t1 and t2 normally develop. (*K–N*) Van Gieson staining of transverse sections through the hindlimbs of newborn mice. (*K*) At the level of the distal end of the tibia, three tendons (t1, t2, t3) are detectable in the wild-type mouse. (*L*) t2 is missing in the absence of *Pax9* (arrow). (*M*) The musculus flexor digitorum (mfd), which is continuous to t2, is located between the musculus tibialis posterior (mtp) and the musculus flexor hallucis (mfh) and is absent in homozygous $Pax9^{lacZ}$ mutants (arrow in *N*). (t1) Tendon of musculus tibialis posterior; (t2) Tendon of musculus flexor digitorum; (t3) Tendon of musculus flexor hallucis. Bars, 100 μm.

embryonic phase of thymus formation. Therefore, it is possible that *Pax9* and *Pax1* regulate different processes during pharyngeal pouch development. Alternatively, if a common set of target genes is postulated, a critical threshold of Pax9/Pax1 protein might be required during early thymus development.

Recently, an ectopic lymphoepithelial structure growing into the lumen of the oral cavity at the level of the developing larynx has been detected in *Pax9*-deficient mouse embryos (C. Egger and T. Boehm, pers. comm.). Experiments are under way to clarify the origin and developmental course of this structure, which could have an immunological function.

Experiments in chick have shown that interactions between neural crest cells and the pharyngeal pouch endoderm are required for thymus development (Le Douarin et al. 1984). This interaction may be affected in *HoxA3*-deficient mice, which lack a thymus (Chisaka and Capecchi 1991). Interestingly, in *HoxA3* mutants, *Pax1* expression in the third pharyngeal pouches is down-regulated (Manley and Capecchi 1995), raising the possibility that *HoxA3* regulates *Pax9* as well. Abnormal neural crest development is believed to cause the absence of thymus and parathyroid in the human congenital disorder DiGeorge syndrome. The localization of the human *PAX9* gene on chromosome 14 (Stapleton et al. 1993) excludes it as a primary gene affected in this syndrome. However, genes affected in DiGeorge syndrome may regulate *Pax9* expression, or, alternatively, are regulated by *Pax9* during the development of thymus and parathyroid glands.

The parathyroid glands and ultimobranchial bodies regulate calcium homeostasis through the release of parathormone and calcitonin, respectively, and are therefore indispensable for the integrity of the skeleton. Although newborn homozygous $Pax9^{lacZ}$ mutants lack both organs, the development of long bones appeared not to be affected (data not shown). Similarly, no defects in long bone formation have been reported in the aparathyroid *HoxA3* knockout mouse (Chisaka and Capecchi 1991). These observations indicate that parathyroid glands and ultimobranchial bodies are not required for

Table 1. *Summary of* Pax9 *expression domains and observed phenotypes in homozygous* Pax9^{lacZ} *mutants*

Origin	Organ	Phenotype
Endoderm	eustachian tube	—
	tonsils	—
	thymus	absent
	parathyroid glands	absent
	ultimobr. bodies	absent
	oral epithelium, pharynx	—
	salivary glands	—
	esophagus, forestomach	—
	trachea	—
	tailgut	—
Mesoderm	processus alaris	absent
	pterygoid process	malformed
	phalanges	digit duplication
	middle foot	malformed
	limb tendons/muscles	absence of m.f.d.
	tail muscles	—
	tongue muscles	—
	intercostal tissue	—
	vertebral column	—
Ectoderm	oral epithelium	—
	tongue epithelium	—
	taste buds	—
	tegmentum	—
	mammillary bodies	—
Neural crest	nasal mesenchyme	—
	palatine, maxilla	cleft palate
	teeth	absent
	coronoid process	absent
	tympanic ring	malformed*
	Reicherts cartilage	malformed*
	hyoid bone	malformed
	thyroid cartilage	malformed
	cricoid cartilage	malformed

Organs are grouped according to the embryonic origins of *Pax9*-expressing structures. Note that cells derived from other germ layers typically also contribute to the formation of a given organ/structure. The phenotypes developed with 100% penetrance if not indicated otherwise. At least eight homozygous *Pax9^{lacZ}* mutants were analyzed for each phenotype. (*) In these organs, malformations did not show full penetrance; 60% (n = 26) of homozygous *Pax^{lacZ}* mutants exhibited a malformed tympanic ring; 3 of 26 homozygous *Pax9^{lacZ}* mutants developed a continuous skeletal element between middle ear and hyoid bone, whereas in the remaining homozygous mutants Reicherts cartilage was absent. (m.f.d.) musculus flexor digitorum; (—) Phenotypic abnormalities were not detected (for details, see text).

long bone development during embryonic and fetal periods.

Skeletal defects

Pax9 and the closely related paralogous gene *Pax1* exhibit a similar expression pattern during the development of the vertebral column. The lack of an obvious phenotype in the vertebral column in *Pax9^{lacZ}* mutants suggests that here the loss of *Pax9* function is rescued by *Pax1*. In double mutant mice lacking both *Pax9* and *Pax1* the vertebral column is more severely affected than in *Pax1* mutants (H. Peters and R. Balling, unpubl.), indicating a redundancy of *Pax9* and *Pax1* in this part of the skeleton.

In the vertebrate limb the establishment of the anterior–posterior axis is controlled by a group of cells located in the posterior limb mesenchyme (for review, see Tickle and Eichele 1994), the zone of polarizing activity (ZPA). A key molecule secreted by the ZPA is Sonic Hedgehog (SHh), which is sufficient to mimic the ZPA when ectopically expressed in the anterior limb mesenchyme (Riddle et al. 1993). Recently, it was shown that in *SHh*-deficient mice *Pax1* expression in the somites is rapidly lost, whereas the expression is not altered in the anterior limb mesenchyme (Chiang et al. 1996). In both domains, *Pax1* and *Pax9* exhibit a similar expression pattern, raising the possibility that *Pax9* might be regulated by SHh in similar ways. In contrast to the ZPA, little is known about the role of the anterior mesenchyme in patterning the anterior–posterior axis of the limb. *Alx-4*, a transcription factor containing a paired-type homeodomain, is specifically expressed in the anterior mesenchyme and the absence of *Alx-4* was shown to cause preaxial digit duplications. It was suggested that *Alx-4* is involved in the repression of an anterior ZPA activity, whose presence might have been the default stage in the limbs of primitive vertebrates (Qu et al. 1997). In fact, in most polydactyly mutants, ectopic expression of *SHh* was found (for review, see Cohn and Tickle 1996). *Pax9* might play a similar role to that of *Alx-4*, however, in *Pax9* mutants, the phenotype of the digits is mild and the absence of *Pax9* affects other anterior regions of the limbs as well. Eventually, the identification of *Pax9* target genes are required to understand the role of *Pax9* during limb development.

Pax9 deficiency also leads to specific skeletal defects during craniofacial development (Table 1). Whereas the affected structures of the skull correlate with the embryonic expression of *Pax9* in the corresponding region, most of the defects seen in the laryngeal cartilages do not. In the latter, *Pax9^{lacZ}* expression was only found in the mesenchyme surrounding Reicherts cartilage while we were not able to detect expression in the precursors of the hyoid and thyroid cartilages. Therefore, we suggest that skeletal malformations in the laryngeal cartilages are caused indirectly, that is, by a failure of interaction with the pharyngeal endoderm. Indeed, tissue recombination studies have indicated that the pharyngeal endoderm is required for cartilage formation of branchial arch-derived mesenchyme in a contact-dependent manner (Hörstadius and Sellman 1946; Epperlein and Lehmann 1975). The severely malformed pharyngeal pouch epithelium of homozygous *Pax9^{lacZ}* mutants may thus explain the skeletal defects of the laryngeal cartilages. However, the mechanisms leading to these defects are presently unclear. Normal pharyngeal epithelium might not only promote cartilage formation in the neighboring mesenchyme, it could also provide positional

information that is required to pattern the laryngeal cartilages.

Not all Pax9 *expression domains are affected in the mutants*

By gross morphological inspection and histological criteria, some organs and structures that express *Pax9* during embryonic development appeared normal in *Pax9*-deficient newborn mice. These include the salivary glands and the epithelia lining the upper digestive tract. Similarly, no abnormalities were detected in the tail, knee, elbow, in intercostal tissue, in the tongue, and in the brain (Table 1, and data not shown). These results may indicate that *Pax9* function is not required in all of its expression domains. However, it should be noted that some of these organs are not yet completely differentiated in newborn mice. In particular, this status applies to the epithelial lining of the upper digestive tract (tongue, oral cavity, pharynx, esophagus, and forestomach), which still expresses *Pax9* in the adult (Peters et al. 1997). Similarly, *Pax9* could play a role in the development of the hypothalamic mammillary body. Recently, it was shown that the lack of *Fkh5,* which is expressed in the mammillary body, leads to disturbed feeding and drinking behavior (Labosky et al. 1997; Wehr et al. 1997). Thus, in some organs, *Pax9* could have essential functions after birth; however, an analysis is precluded by the early death of mutant pups.

Materials and methods

Generation of Pax9-*deficient mice*

A mouse genomic library from 129/Sv mice was screened with a *Pax9* cDNA probe containing the paired box of *Pax9* (Neubüser et al. 1995). Three overlapping phage clones were isolated, which together cover 19.5 kb of genomic DNA containing the start codon and the paired box exon of the *Pax9* gene. A 2.0-kb *Bgl*II–*Eco*RI fragment was cloned into the *Bam*HI–*Eco*RI site of the PGK–*neo* and PGK–*tk* containing vector pPNT (Tybulewicz et al. 1991). In the resulting plasmid (pPax9-1), the *neo* gene and the *tk* gene have the same 5′ → 3′ direction as the *Pax9* gene. A 4.7-kb *Xma*I fragment containing parts of the 5′-untranslated region of the *Pax9*-cDNA was then cloned into the *Xma*I site of pATG–*lacZ* (pPax9-2). The final targeting vector was constructed first by cloning of the upstream 1.0-kb *Xma*I–*Xho*I fragment of pPax9-2 into the *Xho*I site of pPNT containing pPax9-1 to generate pPax9-3. Finally, a 7.2-kb *Xho*I fragment of pPax9-2 containing the major part of the future long arm of the targeting construct fused to the *lacZ* cassette was released and ligated into the same *Xho*I site to generate the targeting vector pPax9-4. The targeting vector (100 µg) was linearized with *Not*I and electroporated into R1 ES cells (Nagy et al. 1993) and selected with G418/gancyclovir as described (Wurst and Joyner 1993). Integrations of the targeting vector via homologous recombination were identified by Southern blot analysis of genomic DNA from resistant ES cell clones with an external probe from the 5′ region of the targeted *Pax9* locus using standard protocols (Wurst and Joyner 1993). Two chimeras obtained by injection of correctly targeted ES cell clones into C57BL/6 blastocysts yielded germ-line transmission. *Pax9*-deficient offspring from both lines exhibited the same phenotype. Genotyping of embryos obtained from heterozygous crosses was performed by PCR with one primer (5′-TTCAGCCGGGCACAGACTTCC-3′, forward) present in the 5′-untranslated region of the *Pax9* cDNA and two allele-specific reverse primers (5′-GCTGGTTCACCTCCCC-GAAGG-3′, $Pax9^{wt}$; and 5′-CGAGTGGCAACATGGAAAT-CGC-3′, $Pax9^{lacZ}$) in one reaction. The resulting 950-bp fragment represents the wild-type *Pax9* allele, whereas the 900-bp fragment was amplified from the $Pax9^{lacZ}$ allele. Chimeras were mated to C57BL/6 mice, and the $Pax9^{lacZ}$ allele was propagated on C57BL/6 genetic background. Offspring from generations F_2–F_6 were used in this study.

X-Gal staining and immunostaining

Whole-mount $Pax9^{lacZ}$ mutant embryos were stained with X-gal for 8–12 hr according to established protocols (Gossler and Zachgo 1993). For sections, X-gal-stained tissue was embedded in paraffin, serially sectioned at 7 µm, and counterstained with Nuclear Red. To completely visualize $Pax9^{lacZ}$ expression, some embryos were dehydrated in methanol and cleared with benzylbenzoate/benzylalcohol.

Pax9-specific polyclonal antibodies (281-IV) were obtained from rabbits immunized with a maltose-binding protein (Guan et al. 1987) fused to the 90 carboxy-terminal amino acids of the murine Pax9 protein according to established protocols (Harlow and Lane 1988). Detection of Pax9 protein in 30-µg protein extracts prepared from the vertebral column of E13.5 embryos by Western blot analysis was performed as described (Peters et al. 1995). After washing, the membranes were incubated with sheep anti-rabbit IgG-alkaline phosphate conjugate (Boehringer Mannheim, Germany), and recognized proteins were visualized by staining with NBT and X-phosphate. Whole-mount immunostainings with HoxB1-specific antibodies (BAbCO, Richmond, USA) were performed as described (Manley and Capecchi 1995).

Tissue recombination

Tissue recombination experiments with dental epithelium and dental mesenchyme from timed E13.5 embryos were carried out as described previously (Kratochwil et al. 1996). Briefly, molar rudiments were dissected from the lower jaws. Tooth mesenchyme and epithelium were separated in 0.1% collagenase at 37°C. For recombination, mesenchyme and epithelium were placed on Nuclepore membrane filters and subsequently cultured for 2 days in vitro and for 11 days more under the kidney capsule of adult mice. Although homozygous $Pax9^{lacZ}$ embryos can be identified because of impaired epithelial development of the incisors, the genotypes of all embryos were determined by PCR analysis. Heterozygous and wild-type embryos served as donors for normal tissue.

Histological procedures and in situ hybridization

For histological analysis and in situ hybridizations, tissues were fixed in 4% paraformaldehyde, dehydrated in isopropanol, and embedded in paraffin. Serial sections at 7 µm were stained with hematoxylin/eosin (H/E) or after Van Gieson. Explanted tissues from recombination experiments were fixed in Bouin's solution. After being embedded in paraffin, they were cut at 7 µm and stained with Azan stain. In situ hybridization on sections was performed as described (Peters et al. 1995; Neubüser et al. 1995). To optimize a comparative expression analysis in the tooth mesenchyme, embryos of one litter were used in parallel for fixation, dehydration, and embedding. Furthermore, frontal sections of wild-type and mutant embryos representing similar anatomical levels were collected on one slide and hybridized simultaneously.

Skeletal staining of cartilage and bone was performed with alcian blue and alizarin red as described (Kessel et al. 1990).

Acknowledgments

We thank R. Grosschedl, M. Nister, and R. Zeller for providing DNA probes and M. Schieweg for technical assistance. We thank C. Egger and T. Boehm for pointing out the presence of the lymphoepithelial structure in the larynx of *Pax9*-deficient mouse embryos. We also thank K. Pfeffer for blastocyst injection, A. Luz for help with histological analysis, and J. Rossant for the vectors pPNT and pATG–*lacZ*, and for the genomic library of 129/Sv mice. We are grateful to R. Maas and R. Grosschedl for providing homozygous $Msx1^{-/-}$ and $Lef1^{-/-}$ mutant embryos, respectively, and to R. Spörle, B. Wilm, and U. Dietz for critical reading of the manuscript. This work was supported by the DFG (Deutsche Forschungsgemeinschaft).

The publication costs of this article were defrayed in part by payment of page charges. This article must therefore be hereby marked ''advertisement'' in accordance with 18 USC section 1734 solely to indicate this fact.

References

Baumgartner, S., D. Bopp, M. Burri, and M. Noll. 1987. Structure of two genes at the gooseberry locus related to the *paired* gene and their spatial expression during embryogenesis. *Genes* & *Dev.* **1:** 1247–1267.

Bopp, D., M. Burri, S. Baumgartner, G. Frigerio, and M. Noll. 1986. Conservation of a large protein domain in the segmentation gene paired and in functionally related genes of *Drosophila*. *Cell* **47:** 1033–1040.

Chalepakis, G., A. Stoykova, J. Wijnholds, P. Tremblay, and P. Gruss. 1993. Pax: Gene regulators in the developing nervous system. *J. Neurobiology* **24:** 1367–1384.

Chen, Y.P., M. Bei, I. Woo, I. Satokata, and R. Maas. 1996. *Msx1* controls inductive signaling in mammalian tooth morphogenesis. *Development* **122:** 3035–3044.

Chiang, C., Y. Litingtung, E. Lee, K.E. Young, J.L. Corden, H. Westphal, and P.A. Beachy. 1996. Cyclopia and defective axial patterning in mice lacking Sonic hedgehog gene function. *Nature* **383:** 407–413.

Chisaka, O. and M. Capecchi. 1991. Regionally restricted developmental defects resulting from the targetted disruption of the mouse homeobox gene hox1.5. *Nature* **350:** 473–479.

Cohn, M.J. and C. Tickle. 1996. Limbs: A model for pattern formation within the vertebrate body plan. *Trends Genet.* **12:** 253–257.

Dahl, E., H. Koseki, and R. Balling. 1997. Pax genes and organogenesis. *Bioessays* **19:** 755–765.

Deutsch, U., G.R. Dressler, and P. Gruss. 1988. *Pax1*, a member of a paired box homologous murine gene family, is expressed in segmented structures during development. *Cell* **53:** 617–625.

Diehl, S.R. and R.P. Erickson. 1997. Genome scan for teratogen-induced clefting susceptibility loci in the mouse: Evidence of both allelic and locus heterogeneity distinguishing cleft lip and cleft palate. *Proc. Natl. Acad. Sci.* **94:** 5231–5236.

Epperlein, H.H. and R. Lehmann. 1975. The ectomesenchymal-endodermal interaction system (EEIS) of *Triturus alpestris* in tissue culture. 2. Observation on the differentiation of visceral cartilage. *Differentiation* **4:** 159–174.

Frohman, M., M. Boyle, and G.R. Martin. 1990. Isolation of the Hox-2.9 gene: Analysis of embryonic expression suggests that positional information along the anterior-posterior axis is specified by mesoderm. *Development* **110:** 589–607.

Gorlin, R.J., M.M. Cohen, and L.S. Levine. 1990. *Syndromes of the head and neck*, 3rd ed. Oxford University Press, New York, NY.

Gossler, A. and J. Zachgo. 1993. Gene and enhancer trap screens in ES cell chimeras. In *Gene targeting: A practical approach* (ed. A.L. Joyner), pp. 181–227. Oxford University Press, New York, NY.

Greene, R.M. and R.M. Pratt. 1976. Developmental aspects of secondary palate formation. *J. Embryol. Exp. Morphol.* **36:** 225–245.

Guan, C., P. Li, P.D. Riggs, and H. Inouye. 1987. Vectors that facilitate the expression and purification of foreign proteins in *Escherichia coli* by fusion to maltose-binding protein. *Gene* **67:** 21–30.

Harlow, E. and D. Lane. 1988. *Antibodies: A laboratory manual*. Cold Spring Harbor Laboratory, Cold Spring Harbor, NY.

Hörstadius, S. and S. Sellman. 1946. Experimentelle Untersuchungen über die Determination des knorpeligen Kopfskelettes bei Urodelen. *Nova Acta R. Soc. Scient. Upsal.* **13:** 1–170.

Jernvall, J., T. Aberg, P. Kettunen, S. Keränen, and I. Thesleff. 1998. The life history of an embryonic signaling center: BMP-4 induces *p21* and is associated with apoptosis in the mouse tooth enamel knot. *Development* **125:** 161–169.

Kessel, M., R. Balling, and P. Gruss. 1990. Variations of cervical vertebrae after expression of a Hox-1.1 transgene in mice. *Cell* **61:** 301–308.

Kratochwil, K., M. Dull, I. Fariñas, J. Galceran, and R. Grosschedl. 1996. *Lef1* expression is activated by BMP-4 and regulates inductive tissue interactions in tooth and hair development. *Genes* & *Dev.* **10:** 1382–1394.

Labosky, P.A., G.E. Winnier, T.L. Jetton, L. Hargett, A.K. Ryan, M.G. Rosenfeld, A.F. Parlow, and B.L.M. Hogan. 1997. The winged helix gene, Mf3, is required for normal development of the diencephalon and midbrain, postnatal growth and milk-ejection reflex. *Development* **124:** 1263–1274.

Le Douarin, L.M., F. Dieterlen-Lievre, and P.D. Oliver. 1984. Ontogeny of primary lymphoid organs and lymphoid stem cells. *Am. J. Anat.* **170:** 261–299.

Lumsden, A.G. 1988. Spatial organization of the epithelium and the role of neural crest cells in the initiation of the mammalian tooth germ. (Suppl.) *Development* **103:** 155–169.

Manley, N.R. and M.R. Capecchi. 1995. The role of Hoxa-3 in mouse thymus and thyroid development. *Development* **121:** 1989–2003.

Mina, M. and E.J. Kollar. 1987. The induction of odontogenesis in non-dental mesenchyme combined with early murine mandibular arch epithelium. *Arch. Oral Biol.* **32:** 123–127.

Murray, J.C. 1995. Face facts: Genes, environment, and clefts. *Am. J. Hum. Genet.* **57:** 227–232.

Nagy, A., J. Rossant, R. Nagy, W. Abramow-Newerly, and J.C. Roder. 1993. Derivation of completely cell culture-derived mice from early-passage embryonic stem cells. *Proc. Natl. Acad. Sci.* **90:** 8424–8428.

Neubüser, A., H. Koseki, and R. Balling. 1995. Characterization and developmental expression of *Pax9*, a paired-box-containing gene related to *Pax1*. *Dev. Biol.* **170:** 701–716.

Neubüser, A., H. Peters, R. Balling, and G. Martin. 1997. Antagonistic interactions between FGF and BMP signaling pathways: A mechanism for positioning the sites of tooth formation. *Cell* **90:** 247–255.

Nornes, S., I. Mikkola, S. Krauss, M. Delghandi, M. Perander, and T. Johansen. 1996. Zebrafish *Pax9* encodes two proteins with distinct C-terminal transactivating domains of different potency negatively regulated by adjacent N-terminal sequences. *J. Biol. Chem.* **271:** 26914–26923.

Peters, H., U. Doll, and J. Niessing. 1995. Differential expression of the chicken *Pax-1* and *Pax-9* gene: In situ hybridiza-

tion and immunohistochemical analysis. *Dev. Dyn.* **203:** 1–16.
Peters, H., G. Schuster, A. Neubüser, T. Richter, H. Höfler, and R. Balling. 1997. Isolation of the *PAX9* cDNA from adult human esophagus. *Mammal. Genome* **8:** 62–64.
Qu, S., K.D. Niswender, Q. Ji, R. van der Meer, D. Keeney, M.A. Magnuson, and R. Wisdom. 1997. Polydactyly and ectopic ZPA formation in *Alx-4* mutant mice. *Development* **124:** 3999–4008.
Riddle, R.D., R.L. Johnson, E. Laufer, and C. Tabin. 1993. *Sonic hedgehog* mediates the polarizing activity of ZPA. *Cell* **75:** 1401–1416.
Satokata, I. and R. Maas. 1994. *Msx-1* deficient mice exhibit cleft palate and abnormalities of craniofacial and tooth development. *Nature Genet.* **6:** 348–356.
Stapleton, P., A. Weith, P. Urbanek, Z. Kozmik, and M. Busslinger. 1993. Chromosomal localisation of seven *Pax* genes and cloning of a novel family member, *Pax9*. *Nature Genet.* **3:** 292–304.
Sulik, K.K., C.S. Cook, and W.S. Webster. 1988. Teratogens and craniofacial malformations: Relationships to cell death. (Suppl.) *Development* **103:** 213–232.
Thesleff, I. and P. Sharpe. 1997. Signalling networks regulating dental development. *Mech. Dev.* **67:** 111–123.
Thorogood, P. 1997. The head and face. In *Embryos, genes, and birth defects* (ed. P. Thorogood), pp. 197–224. John Wiley & Sons, Chichester, UK.
Tickle, C. and G. Eichele. 1994. Vertebrate limb development. *Annu. Rev. Cell. Biol.* **10:** 121–152.
Timmons, P., J. Wallin, P.W.J. Rigby, and R. Balling. 1994. Expression and function of *Pax1* during development of the pectoral girdle. *Development* **120:** 2773–2785.
Tybulewicz, V.L., C.E. Crawford, P.K. Jackson, R.T. Bronson, and R.C. Mulligan. 1991. Neonatal lethality and lymphopenia in mice with a homozygous disruption of the c-abl proto-oncogene. *Cell* **65:** 1153–1163.
Vaahtokari, A., T. Aberg, J. Jernvall, S. Keränen, and I. Thesleff. 1996. The enamel knot is a signalling center in the developing mouse tooth. *Mech. Dev.* **54:** 39–43.
Vainio, S., I. Karavanova, A. Jowett, and I. Thesleff. 1993. Identification of BMP-4 as a signal mediating secondary induction between epithelial and mesenchymal tissues during early tooth development. *Cell* **75:** 45–58.
Van Genderen, C., R.M. Okamura, I. Fariñas, R.G. Quo, T.G. Parslow, L. Bruhn, and R. Grosschedl. 1994. Development of several organs that require inductive epithelial–mesenchymal interactions is impaired in *Lef-1*-deficient mice. *Genes & Dev.* **8:** 2691–2703.
Wallin, J., H. Koseki, K. Imai, K. Moriwaki, N. Miyshita, and R. Balling. 1993. *Pax-9*, a new Pax-gene, maps to mouse chromosome 12. *Mammal. Genome* **4:** 354–358.
Wallin, J., H. Eibel, A. Neubüser, J. Wilting, H. Koseki, and R. Balling. 1996. *Pax1* is expressed during development of the thymus epithelium and is required for normal T-cell maturation. *Development* **122:** 22–30.
Walther, C., J.L. Guenet, D. Simon, U. Deutsch, B. Jostes, M.D. Goulding, D. Plachov, R. Balling, and P. Gruss. 1991. Pax: A multigene family of paired box-containing genes. *Genomics* **11:** 424–434.
Wehr, R., A. Mansouri, T. de Maeyer, and P. Gruss. 1997. Fkh5-deficient mice show dysgenesis in the caudal midbrain and hypothalamic mammillary body. *Development* **124:** 4447–4456.
Wurst, W. and A.L. Joyner. 1993. Production of targeted embryonic stem cell clones. In *Gene targeting: A practical approach* (ed. A.L. Joyner), pp. 33–61. Oxford University Press, New York, NY.